



**NATIONAL ADVISORY COMMITTEE
FOR AERONAUTICS**

TECHNICAL NOTE 3921

APPROXIMATE SOLUTION FOR STREAMLINES ABOUT A LIFTING
ROTOR HAVING UNIFORM LOADING AND OPERATING IN
HOVERING OR LOW-SPEED VERTICAL-ASCENT
FLIGHT CONDITIONS

By Walter Castles, Jr.

Georgia Institute of Technology



Washington

February 1957

FOR REFERENCE

LIBRARY COPY

FEB 18 1957

LANGLEY AERONAUTICAL LABORATORY
LIBRARY, NACA
LANGLEY FIELD, VIRGINIA

NATIONAL ADVISORY COMMITTEE FOR AERONAUTICS

TECHNICAL NOTE 3921

APPROXIMATE SOLUTION FOR STREAMLINES ABOUT A LIFTING
 ROTOR HAVING UNIFORM LOADING AND OPERATING IN
 HOVERING OR LOW-SPEED VERTICAL-ASCENT
 FLIGHT CONDITIONS

By Walter Castles, Jr.



SUMMARY

It is shown that the usual assumption of a uniform vortex cylinder for the wake vortex structure of a uniformly loaded, lifting rotor operating in the hovering or low-speed vertical-ascent flight conditions does not yield useful results for the induced velocities in the region about the periphery of the rotor.

It is then shown that a more realistic approximation for the low-speed flow patterns can be obtained by adding the stream function for the displacement velocity of a disk and the stream function for a ring source coincident with the rim of the rotor to the stream functions for the uniform vortex cylinder and the free-stream velocity. Equations are derived for the relative strengths of the stream functions that are necessary to satisfy certain selected physical conditions.

Tables of the values of the composite stream function are given for hovering and three rates of vertical ascent which cover the helicopter flight range. A method is outlined for using the tabulated values of the stream functions to compute the induced velocity components at any selected locations. In addition, the computed values of the normal component of induced velocity in the plane of a hovering rotor are given for the region extending from 1.1 to 2.0 rotor radii.

The present analysis indicates that there is an appreciable induced upflow in the region around the periphery of a rotor operating in the hovering or low-speed vertical-ascent flight conditions. For a point located at 120 percent radius and in the plane of rotation of a hovering rotor the magnitude of the induced upflow velocity is of the order of 22 percent of the mean induced velocity over the rotor disk. The induced upward velocity component decreases rapidly with increasing distance from the edge of the rotor and, at a point in the vicinity of the center of the second rotor of a twin-rotor helicopter in hovering flight, the upwash has decreased to a value of about $2\frac{1}{2}$ percent of the mean induced velocity over the rotor disk.

INTRODUCTION

Although vortex theory based upon the assumption that the wake vortex system consists of a uniform cylinder as used in references 1 and 2 is useful for computing the approximate values of the normal component of induced velocity over the plane of a lifting rotor for all flight conditions and for computing the whole induced flow field about a lifting rotor for the higher speed flight conditions, this procedure does not afford a reasonable solution for the induced flow field about the periphery of a rotor operating in hovering or very low speed flight. It was therefore decided to investigate the alternate procedure of approximating the flow for hovering and vertical ascent by using a distribution of singularities over the rotor disk.

The present report gives one method of constructing axially symmetric flow patterns similar to those observed about lifting rotors operating in hovering or low-speed vertical ascent. The synthetic flow patterns satisfy certain selected physical requirements so that the results should be sufficiently accurate for estimating the magnitude of the interference-induced velocities on multirotor helicopters and the downwash at fuselages and tail planes.

The present investigation was conducted at the Georgia Institute of Technology under the sponsorship and with the financial assistance of the National Advisory Committee for Aeronautics.

SYMBOLS

R	rotor radius
r	radius of point P(r,z) from rotor axis (fig. 2)
r_0	radius of wake vortex sheet at rotor disk
r_w	wake radius
r_∞	radius of wake vortex sheet a large distance downstream of rotor (or at point of minimum wake radius)
s	distance along wake-vortex-sheet streamline
T	rotor thrust
V	free-stream velocity

V_r	radial component of velocity at point $P(r,z)$
V_z	resultant Z component of velocity at a point $P(r,z)$
v	mean normal component of induced velocity over rotor disk, $\frac{1}{2}\gamma$
v_0	normal component of velocity over rotor disk arising from stream function ψ_0 for actuator-disk displacement velocity
v_{ri}	radial component of induced velocity at a point of radius r_0 on upper surface of rotor inside wake vortex sheet
v_{ro}	radial component of induced velocity at a point of radius r_0 on lower surface of rotor and outside wake vortex sheet
v_s	normal component of velocity at rotor disk arising from stream function ψ_s for uniform distribution of sinks over disk (i.e., induced by a uniform wake vortex cylinder)
z	normal distance of a point P from rotor disk
γ	wake-vortex-sheet strength a large distance downstream of the rotor (or at point of minimum wake radius)
dy/dt	rate of transport of vorticity along wake boundary
θ	angle between streamline at $z = 0$ and $r = r_0$ and normal to rotor disk (see fig. 6)
μ, ϵ	elliptic coordinates
ρ	mass density
ψ	stream function for rotor flow pattern as computed from results of present report
ψ_0	stream function for displacement velocity of actuator disk assumed to be generating the wake vortex rings
ψ_0^*	nondimensional value of ψ_0
ψ_r	stream function for a ring source
$(\psi_r)_t$	strength of ring source located at rotor rim

ψ_r^*	nondimensional value of ψ_r
ψ_s	stream function for a uniform distribution of sinks over rotor disk (i.e., a uniform vortex cylinder)
$(\psi_s)_t$	value of ψ_s for whole sphere
ψ_s^*	nondimensional value of ψ_s
ψ_t	value of ψ on wake boundary
ψ'	stream function for rotor flow pattern as computed using a uniform vortex cylinder for wake vortex system

ANALYSIS

Demonstration of Approximation Involved in Assumption

That Wake Vortex Distribution Consists

of a Uniform Vortex Cylinder

It is shown in reference 3 that the flow induced by a uniform vortex cylinder is identical with the flow induced by a uniform distribution of sinks of proper strength over the end of the cylinder apart from the addition, for the region inside the cylinder, of an axial velocity component equal to the strength of the bounding vortex sheet. A table of the values of the stream function ψ_s for a uniform distribution of sinks over a disk (i.e., a uniform right-circular vortex cylinder) is given in table 17 of the appendix of reference 3. Consequently, it is easier to compute the streamlines for the axially symmetric case where the values of the stream function for the free-stream flow and the flow induced by the vortex cylinder are additive by using the tabulated values of ψ_s than by the method used in reference 2.

The value of the stream function ψ' for the free-stream flow plus the vortex cylinder is thus

$$\psi' = \pi r^2(V + \gamma) - \psi_s \quad (1)$$

for the region inside the wake,

$$\psi' = \pi r^2 V + \psi_s \quad (2)$$

for the region outside the wake, and

$$(\psi_s)_t = 2\pi R^2 v = \pi R^2 \gamma \quad (3)$$

for the full sphere where

ψ_s	value of stream function at r, z for uniform distribution of sinks over rotor disk (i.e., vortex cylinder)
R	rotor radius
r	radius of point from axis of symmetry
z	axial distance of point from rotor plane
V	free-stream velocity
γ	wake-vortex-sheet strength, $2v$
v	normal component of induced velocity at rotor disk

Figure 1(a), plotted from the computed values of ψ' given in table 1(a), shows the streamlines for the vortex cylinder in a free-stream flow for the case where the free-stream velocity V is four times the normal component of the induced velocity v at the rotor disk. It is seen that for this large a ratio of free-stream velocity to induced velocity the assumption of a uniform vortex cylinder for the wake vortex structure gives a reasonable flow pattern except for the slight inflow along the wake boundary. However, for the case where the free-stream velocity V is of the order of magnitude of the induced velocity v there is a large inflow along the wake boundary below the rotor as shown in figure 1(b) for the computed values of ψ' given in table 1(b). For the case of $V = \frac{1}{4} v$ and the case of hovering flight where $V = 0$, the streamlines induced by the uniform vortex cylinder give the inaccurate representation shown plotted in figures 1(c) and 1(d) for the computed values of ψ' given in tables 1(c) and 1(d).

It is obvious from figure 1 that the assumption of a uniform vortex cylinder for the wake vortex structure will not furnish a useful basis for computing the velocity field in the vicinity of the periphery of a lifting rotor unless the free-stream velocity V is several times as large as the mean normal component of the induced velocity v at the rotor disk.

Determination of Useful Approximation for Stream

Function for Vertical Ascent

If consideration is limited to flow patterns generated by the application of successive uniform distributions of impulsive pressure to an actuator disk momentarily coinciding with the rotor, it appears to the author that, on a time-average basis, the actuator disk must have a certain displacement velocity relative to that of the surrounding fluid. The above reasoning suggests that it may be necessary to add the singularity distribution for the displacement velocity of a disk (i.e., a "bound" vortex sheet composed of circular coaxial vortex filaments) to the sink distribution over the rotor disk which represents the effects of the free wake vortices.

In order to simplify the analysis, the only sink distribution that will be used in the present report is a uniform distribution extending over the whole rotor area. This approximation makes it necessary to add a ring source coincident with the rotor rim in order to cancel out the fictitious sink strength within the closed streamline about the periphery of the rotor.

Values of the stream function ψ_0 for the displacement velocity of the actuator disk are given in table 2. These values were computed from the limiting case of the solution for the flow about an oblate spheroid given in reference 4. A table of the values of the stream function for a ring source ψ_r is given in table 6 of the appendix of reference 3.

Let the rotor thrust T be uniformly distributed over the rotor disk of radius R . Let the radius of the wake-boundary streamline at the rotor disk be r_0 and the ultimate wake radius be r_∞ . Let the ultimate wake-vortex-sheet strength be γ and the free-stream velocity be V as shown in figure 2.

Vortex theory demonstrates that, for a lifting surface with uniform loading, the force is equal to the product of the fluid mass density, the area over which the force acts, and the rate of generation of vorticity. In the steady-state system under consideration the rate of generation of vorticity is constant and equal to the rate of transport of vorticity along the wake which is, in turn, equal to the product of the wake-vortex-sheet strength times the wake-vortex-sheet velocity. Thus, using values at a section across the ultimate wake where the sheet strength is the known value γ and the sheet velocity is $V + \frac{1}{2} \gamma$,

$$T = \rho \pi R^2 \gamma \left(V + \frac{1}{2} \gamma \right) \quad (4)$$

or

$$\gamma = -V + \sqrt{V^2 + \frac{2T}{\rho\pi R^2}} \quad (5)$$

The thrust is also equal to the rate of transport of excess momentum across a section of the ultimate wake of radius r_∞ or

$$T = \rho\pi r_\infty^2 \gamma (V + \gamma) \quad (6)$$

It follows from equations (4) and (6) that

$$\left(\frac{r_\infty}{R}\right)^2 = \frac{V + \frac{1}{2}\gamma}{V + \gamma} \quad (7)$$

Let v_0 be the uniform normal component of velocity over the rotor disk that is attributable to the stream function ψ_0 for the displacement velocity of the actuator disk. Let v_s denote the similar velocity component for the stream function ψ_s of the uniform sink distribution (i.e., the vortex cylinder). Then equating the values of ψ on opposite faces of the wake vortex sheet a large distance downstream of the rotor where the sheet strength is the known value γ , the wake radius is the known value r_∞ , the velocity outside the wake is the free-stream value V , and the value of ψ_0 is zero gives

$$\pi r_\infty^2 (V + \gamma) = \pi r_\infty^2 V + 2\pi R^2 v_s - (\psi_r)_t \quad (8)$$

However, for continuity of flow within the closed streamline enclosing the rotor rim the strength $(\psi_r)_t$ of the ring source located at the rotor rim is

$$(\psi_r)_t = 2\pi (R^2 - r_0^2) v_s \quad (9)$$

Solving equations (8) and (9) for v_s

$$v_s = \frac{1}{2} \gamma \left(\frac{r_\infty}{r_0}\right)^2 \quad (10)$$

Equating the value of ψ on the wake boundary at radius r_0 at the rotor disk to the value of ψ at radius r_∞ in the ultimate wake,

$$\pi r_0^2 (V + v_0 + v_s) = \pi r_\infty^2 (V + \gamma) \quad (11)$$

Substituting the value of v_s from equation (10) and solving for v_0 gives

$$v_0 = \left(\frac{r_\infty}{r_0}\right)^2 \left(V + \frac{1}{2} \gamma\right) - V \quad (12)$$

For the larger rates of vertical ascent, say $V \geq \gamma/2$, where the stagnation point on the entering ψ_t streamline is above the plane of the rotor disk, the value of the initial wake radius r_0 is fixed by the requirement that the ψ_t streamline be single valued over the portion of the rotor-disk plane outside the rotor-disk radius. The following procedure may thus be used to compute the values of the stream function outside the wake:

(1) For the given values of the disk loading $\bar{T}/\pi R^2$, free-stream velocity V , and air density ρ , compute the ultimate wake-vortex-sheet strength γ from equation (5).

(2) Compute the value of the square of the ultimate wake-radius ratio $(r_\infty/R)^2$ from equation (7).

(3) Choose three or more initial wake-radius ratios r_0/R covering the range from $\frac{r_0}{R} \approx \sqrt{\frac{r_\infty}{R}}$ to $\frac{r_0}{R} = 1$ and calculate the values of v_0 and v_s for each ratio from equations (10) and (12).

(4) For each initial wake-radius ratio r_0/R compute the values of ψ/ψ_t along a radial line in the plane of the rotor disk for the interval $1 \leq \frac{r}{R} \leq 1.10$. It is to be noted that

$$\psi_s + \psi_r = \pi r_0^2 v_s = \text{Constant}$$

for points in the rotor plane outside the rim of the rotor so that for these plots

$$\psi = \pi r^2 V + \psi_0 + \pi r_0^2 v_s \quad (13)$$

where (taking ψ_0^* from table 2(b))

$$\psi_0 = 2R^2 v_0 \psi_0^* \quad (14)$$

and

$$\psi_t = \pi r_0^2 (V + v_0 + v_s) \quad (15)$$

(It will be noted that if the trial value of r_0/R is too small there will be no intercept of the curve of ψ/ψ_t against r/R with the $\psi/\psi_t = 1$ line as in the top curve of figure 3, whereas if the trial value of r_0/R is too large there will be a double intercept as in the bottom curve. The correct value of r_0/R may thus be determined by plotting the ordinates of the minimum points of the ψ/ψ_t curves against r_0/R and reading the values of r_0/R for the point at which $\psi/\psi_t = 1$.)

(5) Compute the values of v_0 , v_s , and $(\psi_r)_t$ for the given values of V , γ , r_∞/R , and r_0/R .

(6) Then for the region outside the wake

$$\psi = \pi r^2 V + \psi_0 + \psi_s - \psi_r \quad (16)$$

where

$$\psi_0 = 2R^2 v_0 \psi_0^*$$

$$\psi_s = 2R^2 v_s \psi_s^* \quad \text{for upper quadrants}$$

$$\psi_s = 2R^2 v_s (\pi - \psi_s^*) \quad \text{for lower quadrants}$$

$$\psi_r = \frac{(\psi_r)_t}{2\pi} \psi_r^*$$

and the nondimensional values of ψ^* are those given in the aforementioned tables.

For hovering and the smaller rates of vertical ascent where the stagnation point on the entering ψ_t streamline is below the rotor-disk

plane, the value of the initial wake radius r_0 can be found by equating the rate of transport of vorticity (i.e., the product of wake-vortex-sheet strength and wake-vortex-sheet velocity) across the rotor plane at radius r_0 to the value across a section of the ultimate wake. It is shown in the appendix that this procedure gives the solution

$$\left(\frac{r_\infty}{r_0}\right)^4 (1 + \tan^2\theta) = 1 \quad (17)$$

where θ is the angle between the streamline at $z = 0$ and $r = r_0$ and the normal to the rotor disk (see fig. 6) and

$$\tan \theta = \frac{2v_0}{\pi v_s} \frac{r_0}{\sqrt{1 - r_0^2}} \quad (18)$$

The computed value of initial wake radius for hovering ($r_0 = 0.83$) is in good agreement with the experimental value from the smoke-flow study of reference 5.

It is found from numerical computations that it is necessary, for all cases except hovering, to reduce the value of r_∞ slightly (i.e., a few percent) below that given by equation (7) in order to obtain a real solution for r_0 from equations (17) and (18).

For hovering and very small rates of vertical ascent (i.e., $V \leq \frac{1}{4} v$) it is necessary to reduce the value of v_0 given by equation (12) by about 5 percent in order to make the minimum wake radius equal to r_∞ for hovering and in order to eliminate a bulge in the wake-boundary streamlines just below the rotor for the case where $V = \frac{1}{4} v$.

The streamlines computed by the above procedure for the cases of $V = 4v = 2\gamma$, $V = v = \frac{1}{2} \gamma$, $V = \frac{1}{4} v = \frac{1}{8} \gamma$, and $V = 0$ are shown in figure 4. The corresponding tabular values of ψ/ψ_t are given in table 3.

For the present solution, where the wake-vortex-sheet strength and configuration are unspecified except at the rotor disk and in the ultimate wake, there does not appear to be any simple way to obtain an equation for the values of the stream function within the wake. However, it appears to be a good approximation to assume that the axial velocity

component is uniform over each wake cross section since this component is uniform over the sections in the plane of the rotor disk and in the ultimate wake. The tabulated values of ψ for the region inside the wake have therefore been computed using the aforementioned approximation for which

$$\psi = \left(\frac{r}{r_w}\right)^2 \psi_t \quad (19)$$

where r_w is the radius of the wake-boundary streamline as determined from the solution for the external flow.

The axial and radial velocity components V_z and V_r at any point $P(r,z)$ in the flow field may be readily computed from the values of the stream function by means of the relations

$$V_z = \frac{1}{2\pi r} \left(\frac{\partial \psi}{\partial r}\right) \quad (20)$$

and

$$V_r = -\frac{1}{2\pi r} \left(\frac{\partial \psi}{\partial z}\right) \quad (21)$$

Application of Results

Although the whole flow field out to the limits of the tables at $r = \frac{1}{2}z = 2R$ might be mapped for any given flight condition by following the methods given in the previous section, such a procedure is unnecessarily elaborate for most engineering computations. For example, if it is desired to find the axial and radial velocity components at a certain point, say one on a horizontal tail surface, with mean coordinates z' and r' from the rotor hub, the procedure could be as follows:

(1) Calculate the ratio of V/γ for the given helicopter and flight condition using equation (5) to determine the value of γ .

(2) Graphically interpolate between tables 3(a), 3(b), 3(c), and 3(d) for the values of ψ/ψ_t to find the ratios of ψ/ψ_t at V/γ for a set of about nine points (i.e., three values of z'/R and three values of r'/R) enclosing the values of z'/R and r'/R .

(3) Multiply the values of ψ/ψ_t by $\psi_t = \pi R^2 \left(V + \frac{1}{2} \gamma\right)$ to obtain the values of ψ for the nine points.

(4) Interpolate in the set of values of ψ for the three values at $z = z'$ and $r = r_1, r_2,$ and r_3 and for the three values at $r = r'$ and $z = z_1, z_2,$ and z_3 .

(5) Plot ψ against r at $z = z'$ and measure the slope $\partial\psi/\partial r$ at $r = r'$. Then the axial velocity component at z', r' is

$$(V_z)_{z', r'} = \frac{1}{2\pi r'} \left(\frac{\partial\psi}{\partial r} \right)_{z', r'}$$

(6) Plot ψ against z at $r = r'$ and measure the slope $\partial\psi/\partial z$ at $z = z'$. Then the radial velocity component is

$$(V_r)_{z', r'} = - \frac{1}{2\pi r'} \left(\frac{\partial\psi}{\partial z} \right)_{z', r'}$$

For points in the plane of a hovering rotor and outside the closed streamline the axial component of velocity arises solely from the stream function ψ_0 and can thus be expressed in explicit form as

$$V_z = \frac{1}{2\pi r} \left(\frac{\partial\psi_0}{\partial r} \right)_{z=0}$$

or

$$\frac{V_z}{v} = \frac{4v_0}{\pi\gamma} \left(\frac{1}{\sqrt{r^2 - 1}} - \cot^{-1} \sqrt{r^2 - 1} \right) \quad (22)$$

Values of V_z/v calculated from equation (22) for points in the plane of a hovering rotor are given in figure 5 and in table 4 for the region extending from 1.1 to 2.0 rotor radii.

The present analysis indicates that there is an appreciable induced upflow in the region around the periphery of a rotor operating in the hovering or low-speed vertical-ascent flight conditions. For a point located at 120 percent radius and in the plane of rotation of a hovering rotor the magnitude of the induced upflow velocity is of the order of 22 percent of the mean induced velocity over the rotor disk. The induced upward velocity component decreases rapidly with increasing distance from the edge of the rotor and, at a point in the vicinity of the center of the second rotor of a twin-rotor helicopter in hovering flight, the upwash has decreased to a value of about $2\frac{1}{2}$ percent of the mean induced velocity over the rotor disk.

CONCLUDING REMARKS

As in most attempts to obtain an approximate solution of engineering accuracy for a complicated three-dimensional flow pattern, the choice and distribution of the singularities used in the present report are in a sense arbitrary. However, the flow patterns obtained by the method given in the present report satisfy the principal physical requirements and their general form is very similar to that observed in smoke-flow studies of actual rotors. It is therefore thought that the results of the present investigation may be sufficiently accurate for estimating the effects of the interference-induced velocities on multirotor helicopters and for estimating the downwash at helicopter fuselages and tail planes.

The computed value of initial wake radius for hovering ($r_0 = 0.83$) is in good agreement with the experimental value from the smoke-flow study of NACA TN 2474.

Georgia Institute of Technology,
Atlanta, Ga., August 18, 1955.

APPENDIX A

SOLUTION FOR INITIAL WAKE RADIUS r_0 FOR HOVERING

AND VERY LOW RATES OF VERTICAL ASCENT

Let the angle between the normal to the rotor and the tangent to the wake-boundary streamline at $z = 0$ and $r = r_0$ be denoted by θ as shown in figure 6. Let the radial velocity component at a point on the upper surface of the rotor and just inside the wake boundary be v_{r1} and the radial velocity component on the lower surface just outside the wake boundary be v_{r0} . Then the difference in radial velocity component Δv_r across the wake vortex sheet at r_0 is

$$\Delta v_r = v_{r1} - v_{r0} \quad (A1)$$

The discontinuity in radial velocity Δv_r at r_0 arises solely from the stream function ψ_0 since the radial velocity components arising from ψ_s and ψ_r are continuous at this point. Thus the value of Δv_r is equal to twice the radial velocity component at r_0 that arises from ψ_0 .

Thus,

$$\frac{1}{2} \Delta v_r = \frac{1}{2\pi r} \frac{\partial \psi_0}{\partial z} \quad (A2)$$

However, from reference 4 the value of ψ_0 in elliptic coordinates is

$$\psi_0 = 2v_0 (1 - \mu^2)(\epsilon^2 + 1) \left(\frac{\epsilon}{\epsilon^2 + 1} - \cot^{-1} \epsilon \right) \quad (A3)$$

where

$$\mu \epsilon = z \quad (A4)$$

and

$$\sqrt{1 - \mu^2} \sqrt{\epsilon^2 + 1} = r \quad (A5)$$

It follows from equations (A1) to (A5) that

$$\Delta v_r = \frac{4v_o r_o}{\pi \sqrt{1 - r_o^2}} \quad (A6)$$

For the singularity distributions used in the present report the difference in the normal velocity component across the wake vortex sheet at r_o is merely $2v_s$. Thus, equating the ratios of corresponding sides of the similar triangles formed by the velocity vectors on opposite sides of the wake vortex sheet at r_o , solving for $V + v_o$ in terms of v_{r1} , v_{r0} , and v_s , and substituting the result back in the expression for $\tan \theta$ give

$$\tan \theta = \frac{\Delta v_r}{2v_s} = \frac{2v_o}{\pi v_s} \left(\frac{r_o}{\sqrt{1 - r_o^2}} \right) \quad (A7)$$

The wake-vortex-sheet strength γ at $z = 0$ and $r = r_o$ is the difference in velocities on opposite sides of the sheet or

$$\begin{aligned} (\gamma)_{z=0} &= \left[(V + v_o + v_s) - (V + v_o - v_s) \right] \sec \theta \\ &= 2v_s \sec \theta \end{aligned} \quad (A8)$$

and the vortex-sheet velocity ds/dt is half the sum of the velocities on opposite sides of the sheet or

$$\begin{aligned} \left(\frac{ds}{dt} \right)_{z=0} &= \frac{1}{2} \left[(V + v_o + v_s) + (V + v_o - v_s) \right] \sec \theta \\ &= (V + v_o) \sec \theta \end{aligned} \quad (A9)$$

The rate of transport of vorticity (dy/dt) across the plane of the rotor at r_o is equal to the product of the sheet strength and sheet velocity or from equations (A8) and (A9)

$$\left(\frac{dy}{dt} \right)_{r_o} = 2v_s (V + v_o) (1 + \tan^2 \theta) \quad (A10)$$

Equating the rate of transport of vorticity across the rotor plane to the known value $\gamma\left(V + \frac{1}{2}\gamma\right)$ across a section of the ultimate wake and using equations (10) and (12) to eliminate v_s and v_o give

$$\left(\frac{r_\infty}{r_o}\right)^4 (1 + \tan^2\theta) = 1 \quad (A11)$$

Equations (A7) and (A11) can be solved for the value of r_o for any given flight condition by use of equations (5), (7), (10), and (12).

Figure 7 gives the resulting computed values of r_o for the smaller rates of vertical ascent.

REFERENCES

1. Knight, Montgomery, and Hefner, Ralph A.: Static Thrust Analysis of the Lifting Airscrew. NACA TN 626, 1937.
2. Castles, Walter, Jr., and De Leeuw, Jacob Henri: The Normal Component of the Induced Velocity in the Vicinity of a Lifting Rotor and Some Examples of Its Application. NACA Rep. 1184, 1954.
3. Küchemann, Dietrich, and Weber, Johanna: Aerodynamics of Propulsion. Section 3-6. First ed., McGraw-Hill Book Co., Inc., 1953, pp. 55-57.
4. Lamb, Horace: Hydrodynamics. Sixth ed., Dover Pub., 1945, pp. 142-145.
5. Castles, Walter, Jr., and Gray, Robin B.: Empirical Relation Between Induced Velocity, Thrust, and Rate of Descent of a Helicopter Rotor as Determined by Wind-Tunnel Tests on Four Model Rotors. NACA TN 2474, 1951.

TABLE 1.- VALUES OF STREAM FUNCTION FOR WAKE CONSISTING
OF A UNIFORM VORTEX CYLINDER

$$(a) \quad V = 4v = 2\gamma$$

$\frac{z}{R}$	ψ/ψ_t for values of r/R of -										
	0	0.2	0.4	0.6	0.8	1.0	1.2	1.4	1.6	1.8	2.0
	Above plane of rotor										
0	0	0.040	0.160	0.360	0.640	1.000	1.352	1.768	2.248	2.792	3.400
.2	0	.038	.153	.343	.605	.932	1.307	1.734	2.219	2.767	3.378
.4	0	.037	.148	.330	.581	.897	1.272	1.703	2.193	2.743	3.357
.6	0	.036	.143	.320	.564	.874	1.245	1.677	2.169	2.722	3.337
.8	0	.035	.139	.313	.553	.858	1.226	1.656	2.149	2.703	3.320
1.0	0	.034	.137	.308	.545	.847	1.213	1.642	2.133	2.687	3.304
1.2	0	.034	.135	.304	.539	.839	1.203	1.631	2.122	2.675	3.290
1.4	0	.033	.134	.301	.534	.833	1.196	1.622	2.112	2.664	3.279
1.6	0	.033	.133	.299	.530	.827	1.189	1.614	2.103	2.655	3.270
1.8	0	.033	.132	.297	.527	.823	1.183	1.607	2.096	2.647	3.262
2.0	0	.032	.131	.296	.525	.819	1.178	1.601	2.089	2.639	3.255
	Below plane of rotor										
0	0	0.040	0.160	0.360	0.640	1.000	1.352	1.768	2.248	2.792	3.400
-.2	0	.042	.166	.377	.674	1.068	1.397	1.802	2.277	2.817	3.422
-.4	0	.043	.172	.390	.699	1.103	1.432	1.833	2.303	2.840	3.443
-.6	0	.044	.177	.400	.716	1.126	1.459	1.859	2.326	2.861	3.462
-.8	0	.045	.180	.407	.727	1.142	1.478	1.879	2.347	2.880	3.480
-1.0	0	.045	.183	.412	.735	1.153	1.491	1.894	2.363	2.896	3.496
-1.2	0	.046	.185	.416	.741	1.160	1.500	1.905	2.374	2.909	3.509
-1.4	0	.047	.186	.419	.746	1.167	1.508	1.914	2.384	2.919	3.520
-1.6	0	.047	.187	.421	.749	1.173	1.514	1.921	2.392	2.928	3.529
-1.8	0	.047	.187	.423	.753	1.177	1.521	1.928	2.400	2.936	3.537
-2.0	0	.047	.189	.424	.755	1.181	1.526	1.935	2.407	2.944	3.545

TABLE 1.- VALUES OF STREAM FUNCTION FOR WAKE CONSISTING
OF A UNIFORM VORTEX CYLINDER - Continued

$$(b) \quad V = v = \frac{1}{2} \gamma$$

$\frac{z}{R}$	ψ/ψ_t for values of r/R of -										
	0	0.2	0.4	0.6	0.8	1.0	1.2	1.4	1.6	1.8	2.0
	Above plane of rotor										
0	0	0.041	0.159	0.360	0.640	1.000	1.220	1.480	1.780	2.120	2.500
.2	0	.036	.143	.318	.554	.829	1.108	1.395	1.708	2.057	2.445
.4	0	.033	.129	.285	.492	.742	1.019	1.317	1.643	1.999	2.393
.6	0	.030	.118	.259	.450	.685	.952	1.252	1.584	1.946	2.344
.8	0	.028	.108	.242	.422	.645	.905	1.201	1.533	1.898	2.299
1.0	0	.026	.102	.229	.403	.618	.873	1.165	1.493	1.859	2.259
1.2	0	.025	.097	.220	.388	.599	.849	1.138	1.464	1.827	2.226
1.4	0	.023	.094	.212	.376	.583	.830	1.115	1.439	1.801	2.199
1.6	0	.023	.093	.207	.366	.568	.814	1.096	1.418	1.779	2.177
1.8	0	.023	.091	.202	.358	.557	.798	1.079	1.399	1.758	2.156
2.0	0	.022	.088	.199	.352	.548	.785	1.063	1.382	1.739	2.137
	Below plane of rotor										
0	0	0.039	0.160	0.360	0.640	1.000	1.220	1.480	1.780	2.120	2.500
-.2	0	.044	.176	.401	.726	1.170	1.332	1.565	1.852	2.182	2.554
-.4	0	.047	.191	.435	.788	1.258	1.421	1.643	1.917	2.241	2.607
-.6	0	.050	.202	.460	.829	1.315	1.488	1.708	1.976	2.294	2.656
-.8	0	.052	.211	.478	.858	1.355	1.535	1.759	2.027	2.341	2.700
-1.0	0	.053	.218	.490	.877	1.382	1.567	1.795	2.067	2.381	2.740
-1.2	0	.055	.222	.500	.891	1.401	1.591	1.822	2.095	2.413	2.774
-1.4	0	.057	.226	.508	.904	1.417	1.610	1.845	2.121	2.438	2.801
-1.6	0	.057	.227	.513	.914	1.431	1.626	1.864	2.142	2.461	2.823
-1.8	0	.057	.229	.517	.922	1.442	1.642	1.881	2.161	2.481	2.844
-2.0	0	.058	.232	.521	.928	1.452	1.655	1.897	2.178	2.501	2.863

TABLE 1.- VALUES OF STREAM FUNCTION FOR WAKE CONSISTING
OF A UNIFORM VORTEX CYLINDER - Continued

$$(c) \quad V = \frac{1}{4} v = \frac{1}{8} \gamma$$

$\frac{z}{R}$		ψ/ψ_t for values of r/R of -									
		0	0.2	0.4	0.6	0.8	1.0	1.2	1.4	1.6	1.8
Above plane of rotor											
0	0	0.041	0.159	0.359	0.640	1.000	1.088	1.192	1.312	1.448	1.600
.2	0	.034	.134	.293	.502	.727	.909	1.056	1.197	1.348	1.513
.4	0	.029	.111	.240	.403	.587	.767	.931	1.092	1.254	1.429
.6	0	.023	.093	.199	.337	.495	.660	.827	.998	1.170	1.350
.8	0	.021	.078	.171	.291	.432	.583	.746	.917	1.093	1.279
1.0	0	.018	.068	.151	.261	.388	.532	.687	.853	1.030	1.215
1.2	0	.016	.060	.135	.238	.358	.494	.644	.807	.979	1.162
1.4	0	.013	.055	.123	.217	.332	.464	.608	.767	.938	1.118
1.6	0	.013	.052	.115	.202	.309	.438	.578	.733	.902	1.083
1.8	0	.013	.050	.107	.189	.292	.413	.550	.703	.869	1.050
2.0	0	.011	.045	.102	.179	.276	.392	.524	.675	.839	1.019
Below plane of rotor											
0	0	0.039	0.161	0.360	0.640	1.000	1.088	1.192	1.312	1.448	1.600
-.2	0	.046	.186	.427	.777	1.272	1.266	1.327	1.427	1.547	1.687
-.4	0	.051	.209	.480	.876	1.412	1.409	1.452	1.531	1.642	1.771
-.6	0	.056	.227	.521	.943	1.504	1.516	1.556	1.625	1.726	1.850
-.8	0	.059	.242	.549	.988	1.568	1.592	1.637	1.707	1.802	1.921
-1.0	0	.062	.252	.569	1.019	1.611	1.643	1.696	1.770	1.865	1.985
-1.2	0	.064	.260	.584	1.042	1.642	1.681	1.739	1.816	1.916	2.038
-1.4	0	.067	.265	.597	1.061	1.667	1.712	1.775	1.857	1.957	2.081
-1.6	0	.067	.268	.605	1.078	1.690	1.737	1.805	1.890	1.993	2.117
-1.8	0	.667	.270	.612	1.090	1.708	1.763	1.833	1.920	2.026	2.150
-2.0	0	.069	.275	.617	1.100	1.723	1.783	1.859	1.948	2.056	2.181

TABLE 1.- VALUES OF STREAM FUNCTION FOR WAKE CONSISTING
OF A UNIFORM VORTEX CYLINDER - Concluded

(d) $V = 0$

$\frac{z}{R}$	Ψ/Ψ_t for values of r/R of -										
	0	0.2	0.4	0.6	0.8	1.0	1.2	1.4	1.6	1.8	2.0
Above plane of rotor											
0	0	0.041	0.159	0.360	0.640	1.000	1.000	1.000	1.000	1.000	1.000
.2	0	.32	.127	.277	.468	.659	.777	.831	.856	.875	.891
.4	0	.025	.099	.210	.344	.434	.598	.675	.726	.757	.786
.6	0	.019	.076	.159	.261	.369	.464	.544	.608	.652	.687
.8	0	.016	.057	.124	.204	.290	.369	.442	.506	.557	.598
1.0	0	.013	.044	.099	.165	.235	.305	.369	.426	.477	.519
1.2	0	.009	.035	.079	.137	.197	.258	.315	.369	.414	.452
1.4	0	.006	.029	.064	.111	.165	.220	.270	.318	.363	.398
1.6	0	.006	.025	.054	.092	.137	.188	.232	.277	.318	.353
1.8	0	.006	.022	.044	.076	.114	.156	.197	.239	.277	.312
2.0	0	.003	.016	.038	.064	.095	.130	.165	.204	.239	.274
Below plane of rotor											
0	0	0.041	0.161	0.360	0.640	1.000	1.000	1.000	1.000	1.000	1.000
-.2	0	.048	.193	.443	.812	1.341	1.223	1.169	1.144	1.125	1.109
-.4	0	.055	.221	.510	.936	1.156	1.402	1.325	1.274	1.242	1.214
-.6	0	.061	.244	.561	1.739	1.631	1.535	1.456	1.392	1.347	1.312
-.8	0	.064	.263	.596	1.796	1.710	1.631	1.558	1.494	1.443	1.402
-1.0	0	.067	.276	.621	1.834	1.764	1.694	1.631	1.573	1.523	1.481
-1.2	0	.071	.285	.640	1.863	1.803	1.742	1.685	1.631	1.586	1.548
-1.4	0	.074	.291	.656	1.889	1.834	1.780	1.729	1.682	1.637	1.602
-1.6	0	.074	.295	.666	1.908	1.863	1.812	1.768	1.723	1.682	1.647
-1.8	0	.074	.298	.675	1.924	1.885	1.844	1.803	1.761	1.723	1.688
-2.0	0	.077	.304	.682	1.936	1.904	1.869	1.834	1.796	1.761	1.726

TABLE 2.- VALUES OF STREAM FUNCTION ψ_0^* FOR
 DISPLACEMENT VELOCITY OF A DISK
 (a) $r/R = 0$ to 2.0 ; $z/R = 0$ to 2.0

$\frac{z}{R}$	ψ_0^* for values of r/R of -										
	0	0.2	0.4	0.6	0.8	1.0	1.2	1.4	1.6	1.8	2.0
0	0	0.063	0.251	0.565	1.005	1.571	0.755	0.579	0.478	0.410	0.362
.2	0	.047	.184	.395	.632	.740	.652	.540	.459	.397	.355
.4	0	.033	.128	.266	.407	.492	.495	.457	.410	.370	.332
.6	0	.023	.088	.182	.274	.342	.372	.369	.349	.327	.305
.8	0	.016	.061	.124	.191	.244	.279	.294	.294	.283	.271
1.0	0	.011	.042	.085	.137	.180	.213	.232	.240	.239	.237
1.2	0	.008	.030	.063	.100	.135	.164	.185	.198	.203	.204
1.4	0	.006	.022	.047	.075	.103	.128	.148	.164	.173	.175
1.6	0	.004	.017	.034	.057	.080	.101	.120	.131	.144	.152
1.8	0	.003	.013	.027	.044	.063	.081	.097	.111	.121	.130
2.0	0	.002	.010	.021	.035	.050	.065	.080	.092	.103	.111

TABLE 2.- VALUES OF STREAM FUNCTION ψ_0^* FOR

DISPLACEMENT VELOCITY OF A DISK - Concluded

(b) $r/R = 1.01$ to 1.10 ; $z/R = 0$

$\frac{r}{R}$	ψ_0^*
1.01	1.3168
1.02	1.2269
1.03	1.1630
1.04	1.1125
1.05	1.0700
1.06	1.0334
1.07	1.0012
1.08	.9724
1.09	.9463
1.10	.9226

TABLE 3.- VALUES OF THE STREAM FUNCTION DETERMINED BY
APPROXIMATION GIVEN IN PRESENT PAPER

$$(a) \quad V = 4v = 2\gamma$$

$\frac{z}{R}$	ψ/ψ_t for values of r/R of -										
	0	0.2	0.4	0.6	0.8	1.0	1.2	1.4	1.6	1.8	2.0
	Above plane of rotor										
0	0	0.040	0.160	0.360	0.640	1.000	1.335	1.747	2.225	2.767	3.374
.2	0	.038	.153	.342	.603	.925	1.295	1.718	2.200	2.746	3.356
.4	0	.037	.147	.329	.578	.891	1.262	1.690	2.177	2.726	3.338
.8	0	.035	.139	.311	.550	.853	1.219	1.648	2.138	2.690	3.305
1.2	0	.034	.134	.302	.537	.836	1.198	1.624	2.114	2.665	3.280
1.6	0	.033	.132	.298	.528	.824	1.185	1.609	2.097	2.648	3.262
2.0	0	.032	.131	.295	.523	.817	1.175	1.597	2.084	2.634	3.248
	Below plane of rotor										
0	0	0.040	0.160	0.360	0.640	1.000	1.335	1.747	2.225	2.767	3.374
-.2	0	.042	.169	.381	.677	1.039	1.370	1.774	2.248	2.788	3.392
-.4	0	.043	.174	.391	.694	1.063	1.396	1.798	2.269	2.807	3.409
-.8	0	.045	.181	.407	.724	1.089	1.430	1.834	2.303	2.838	3.439
-1.2	0	.046	.185	.416	.740	1.103	1.446	1.853	2.324	2.861	3.462
-1.6	0	.047	.187	.420	.747	1.112	1.456	1.865	2.338	2.875	3.478
-2.0	0	.047	.188	.423	.753	1.118	1.465	1.875	2.349	2.888	3.490

TABLE 3.- VALUES OF STREAM FUNCTION DETERMINED BY
APPROXIMATION GIVEN IN PRESENT PAPER - Continued

$$(b) \quad V = v = \frac{1}{2} \gamma$$

$\frac{z}{R}$		ψ/ψ_t for values of r/R of -									
		0	0.2	0.4	0.6	0.8	1.0	1.2	1.4	1.6	1.8
Above plane of rotor											
0	0	0.042	0.164	0.370	0.659	{1.020 1.030	1.143	1.382	1.670	2.002	2.376
.2	0	.036	.145	.321	.554	.811	1.058	1.322	1.621	1.959	2.340
.4	0	.032	.129	.283	.485	.721	.980	1.260	1.571	1.917	2.302
.8	0	.027	.107	.236	.411	.626	.876	1.163	1.484	1.840	2.232
1.2	0	.024	.095	.214	.378	.582	.826	1.107	1.427	1.783	2.175
1.6	0	.022	.090	.202	.358	.556	.795	1.072	1.388	1.744	2.136
2.0	0	.021	.086	.195	.345	.538	.771	1.045	1.359	1.712	2.104
Below plane of rotor											
0	0	0.041	0.165	0.371	0.659	{1.020 1.010	1.143	1.382	1.670	2.002	2.376
-.2	0	.044	.176	.397	.705	1.032	1.204	1.433	1.716	2.042	2.412
-.4	0	.047	.189	.425	.756	1.062	1.245	1.475	1.753	2.078	2.444
-.8	0	.052	.206	.464	.826	1.098	1.296	1.533	1.812	2.134	2.499
-1.2	0	.054	.216	.487	.866	1.116	1.320	1.563	1.847	2.172	2.540
-1.6	0	.055	.221	.498	.885	1.130	1.336	1.583	1.870	2.197	2.566
-2.0	0	.057	.226	.510	.906	1.141	1.351	1.601	1.889	2.219	2.588

TABLE 3.- VALUES OF STREAM FUNCTION DETERMINED BY
APPROXIMATION GIVEN IN PRESENT PAPER - Continued

$$(c) \quad v = \frac{1}{4} \omega = \frac{1}{8} \gamma$$

$\frac{z}{R}$	ψ/ψ_t for values of r/R of -										
	0	0.2	0.4	0.6	0.8	1.0	1.2	1.4	1.6	1.8	2.0
	Above plane of rotor										
0	0	0.052	0.204	0.460	0.818	{ 1.153 1.280	0.986	1.038	1.129	1.246	1.387
.2	0	.041	.162	.352	.583	.772	.868	.957	1.061	1.187	1.336
.4	0	.032	.127	.269	.438	.601	.738	.862	.989	1.128	1.283
.6	0	.025	.100	.213	.348	.494	.634	.774	.917	1.067	1.230
.8	0	.022	.081	.175	.292	.422	.558	.702	.852	1.009	1.179
1.0	0	.018	.068	.149	.256	.376	.507	.648	.798	.959	1.132
1.2	0	.016	.059	.132	.229	.342	.469	.609	.758	.918	1.091
1.6	0	.012	.050	.110	.193	.295	.416	.548	.695	.856	1.029
2.0	0	.010	.044	.098	.172	.266	.376	.504	.647	.805	.979
	Below plane of rotor										
0	0	0.052	0.204	0.460	0.818	{ 1.153 1.026	0.986	1.038	1.129	1.246	1.387
-.2	0	.052	.207	.465	.826	1.012	1.038	1.094	1.183	1.296	1.432
-.4	0	.054	.216	.487	.865	1.026	1.070	1.136	1.224	1.339	1.471
-.6	0	.058	.232	.523	.929	1.038	1.097	1.169	1.259	1.372	1.507
-.8	0	.062	.247	.555	.988	1.049	1.114	1.194	1.288	1.403	1.536
-1.0	0	.064	.256	.577	1.001	1.057	1.124	1.209	1.309	1.425	1.562
-1.2	0	.066	.263	.592	1.004	1.060	1.132	1.220	1.321	1.443	1.583
-1.6	0	.071	.284	.640	1.013	1.073	1.145	1.237	1.343	1.468	1.612
-2.0	0	.075	.300	.675	1.021	1.084	1.162	1.258	1.367	1.494	1.636

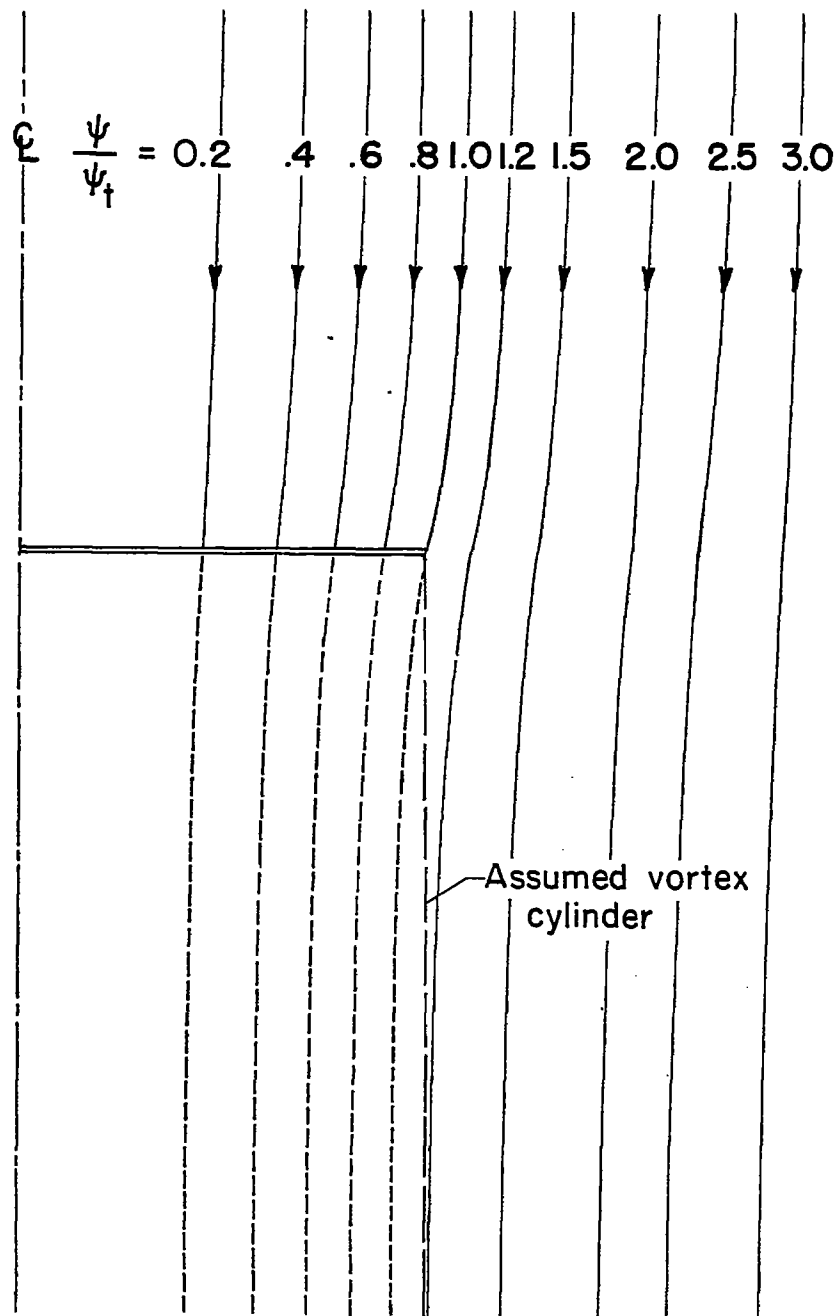
TABLE 3.- VALUES OF STREAM FUNCTION DETERMINED BY APPROXIMATION GIVEN IN PRESENT PAPER - Concluded

(d) $v = 0$

$\frac{z}{R}$		ψ/ψ_t for values of r/R of -									
		0	0.2	0.4	0.6	0.8	1.0	1.2	1.4	1.6	1.8
Above plane of rotor											
0	0	0.058	0.225	0.507	0.904	{1.200 1.413	0.845	0.768	0.723	0.694	0.673
.2	0	.043	.168	.362	.586	.715	.711	.677	.648	.628	.618
.4	0	.031	.121	.252	.392	.500	.551	.565	.564	.559	.555
.6	0	.022	.087	.178	.276	.363	.422	.457	.478	.487	.493
.8	0	.018	.062	.128	.203	.272	.326	.368	.399	.419	.432
1.0	0	.012	.044	.094	.155	.212	.262	.302	.333	.357	.376
1.2	0	.009	.033	.073	.128	.170	.214	.253	.285	.308	.326
1.4	0	.006	.026	.056	.096	.138	.178	.212	.243	.269	.286
1.6	0	.006	.022	.046	.077	.111	.148	.180	.206	.233	.253
1.8	0	.005	.019	.036	.062	.090	.121	.149	.177	.200	.221
2.0	0	.001	.014	.030	.050	.073	.099	.123	.148	.170	.192
Below plane of rotor											
0	0	0.057	0.226	0.510	0.906	{1.200 .987	0.845	0.768	0.723	0.694	0.673
-.2	0	.069	.277	.623	.995	.955	.886	.825	.782	.748	.723
-.4	0	.075	.300	.676	.993	.959	.910	.864	.822	.794	.765
-.6	0	.076	.304	.685	.992	.965	.932	.894	.856	.828	.803
-.8	0	.075	.300	.676	.994	.971	.946	.917	.886	.859	.834
-1.0	0	.074	.296	.666	.994	.976	.953	.930	.906	.881	.861
-1.2	0	.073	.292	.657	.995	.978	.959	.939	.917	.899	.882
-1.4	0	.061	.244	.548	.975	.982	.964	.947	.930	.912	.896
-1.6	0	.054	.216	.487	.865	.989	.970	.955	.938	.923	.910
-1.8	0	.047	.187	.420	.747	.995	.980	.965	.950	.935	.922
-2.0	0	.040	.160	.360	.640	1.000	.988	.976	.962	.949	.935

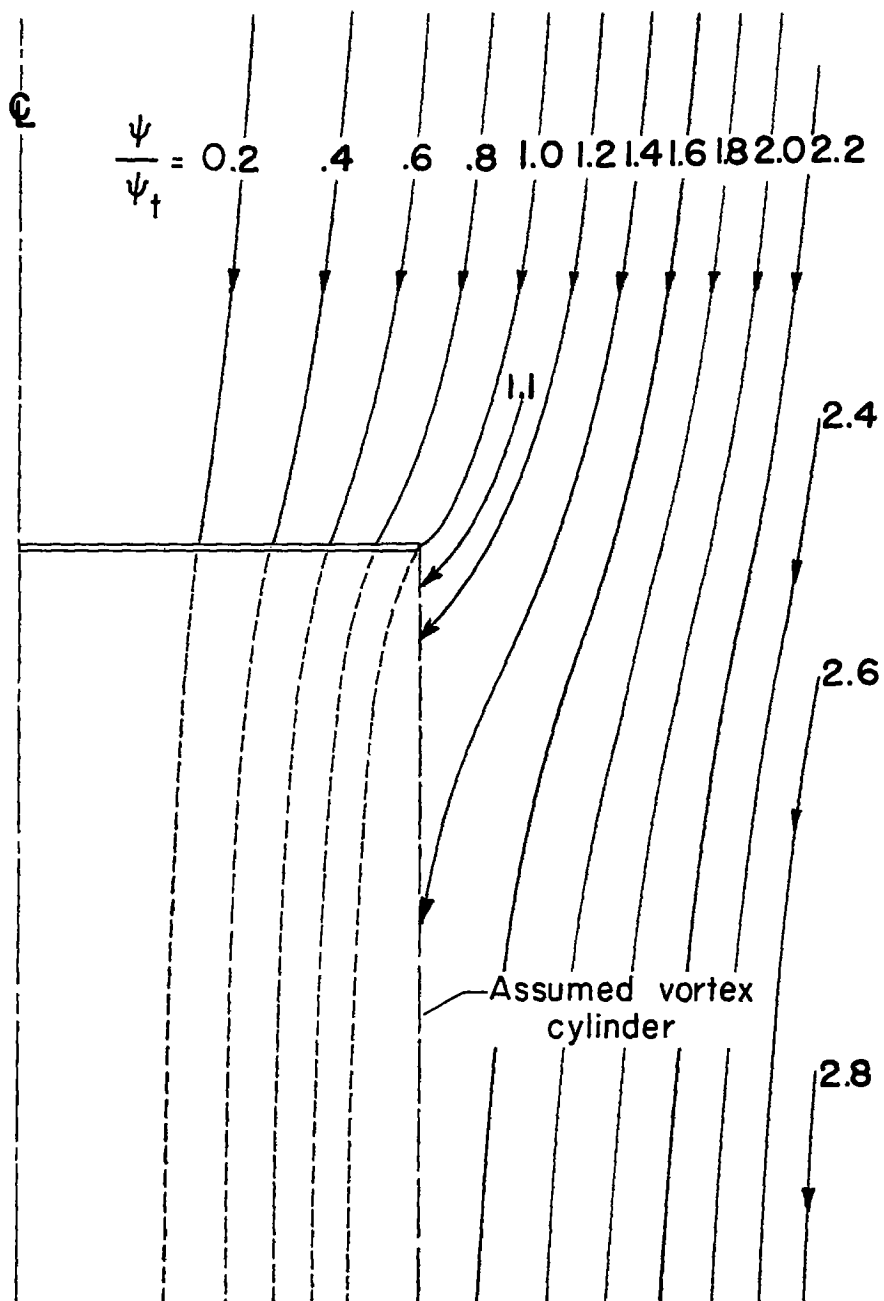
TABLE 4.- NORMAL COMPONENT OF THE INDUCED UPFLOW
VELOCITY IN PLANE OF ROTATION OF A UNIFORMLY
LOADED, HOVERING ROTOR

$\frac{r}{R}$	$\frac{V_z}{V}$
1.1	-0.44052
1.2	-.22110
1.4	-.09519
1.6	-.04865
1.8	-.03351
2.0	-.02434



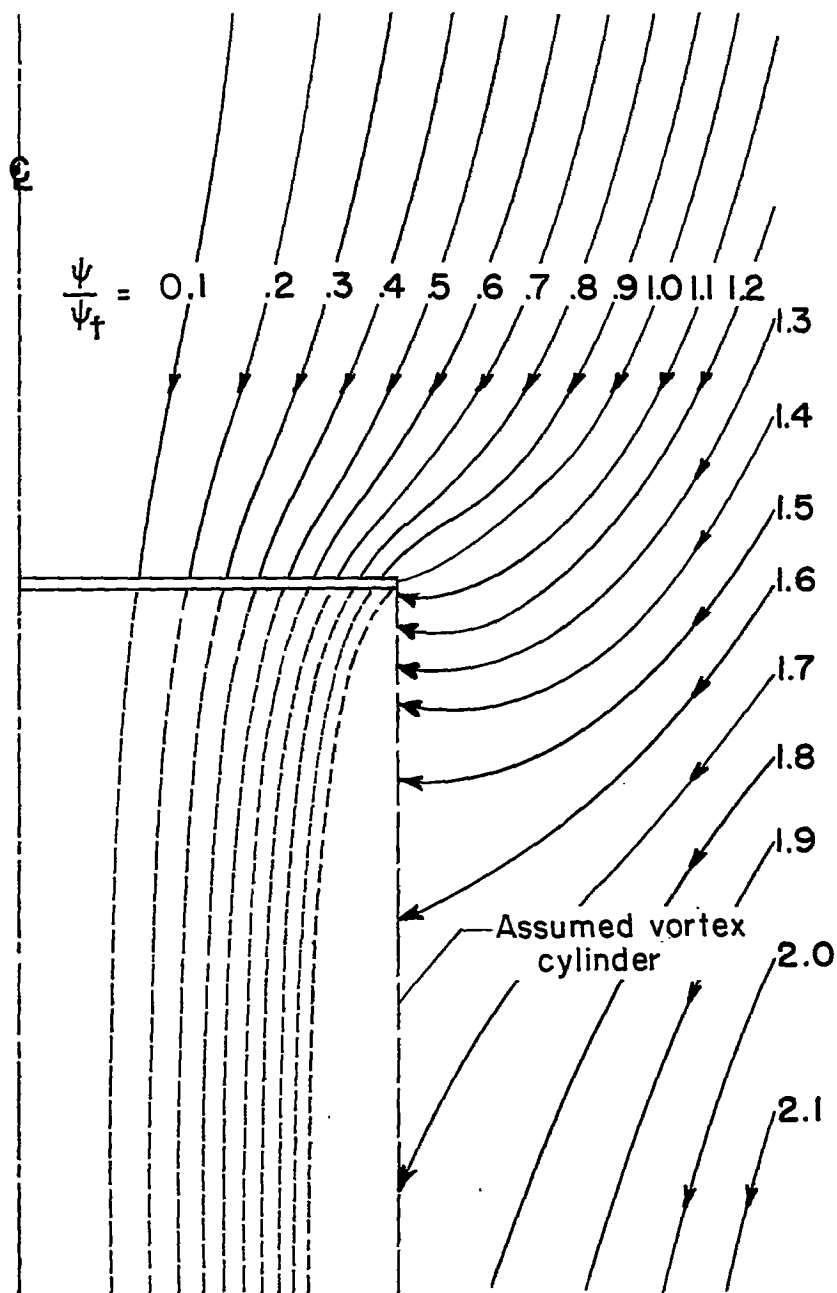
(a) $V = 4v = 2\gamma$.

Figure 1.- Streamlines for wake consisting of uniform vortex cylinder.



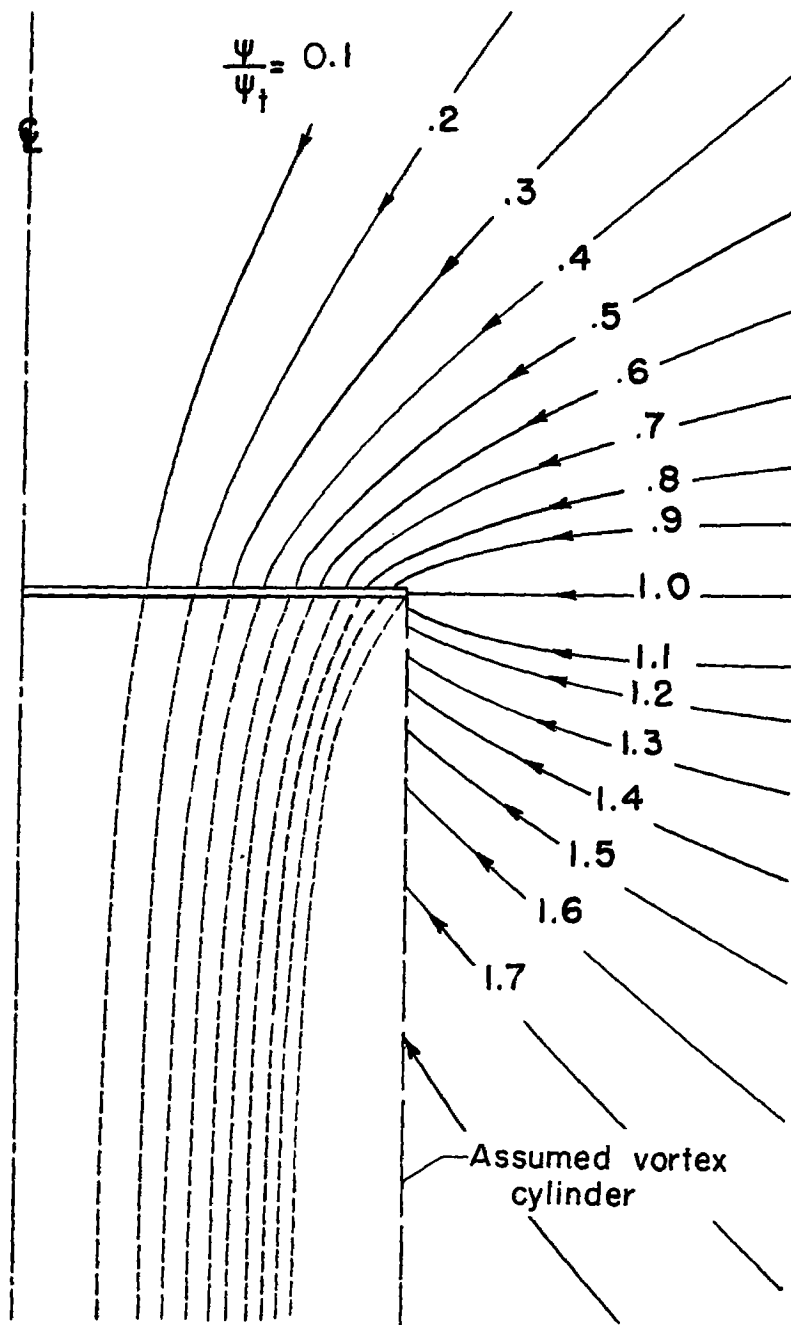
(b) $V = v = \frac{1}{2} \gamma.$

Figure 1.- Continued.



(c) $V = \frac{1}{4} v = \frac{1}{8} \gamma.$

Figure 1.- Continued.



(d) $V = 0$ (hovering).

Figure 1.- Concluded.

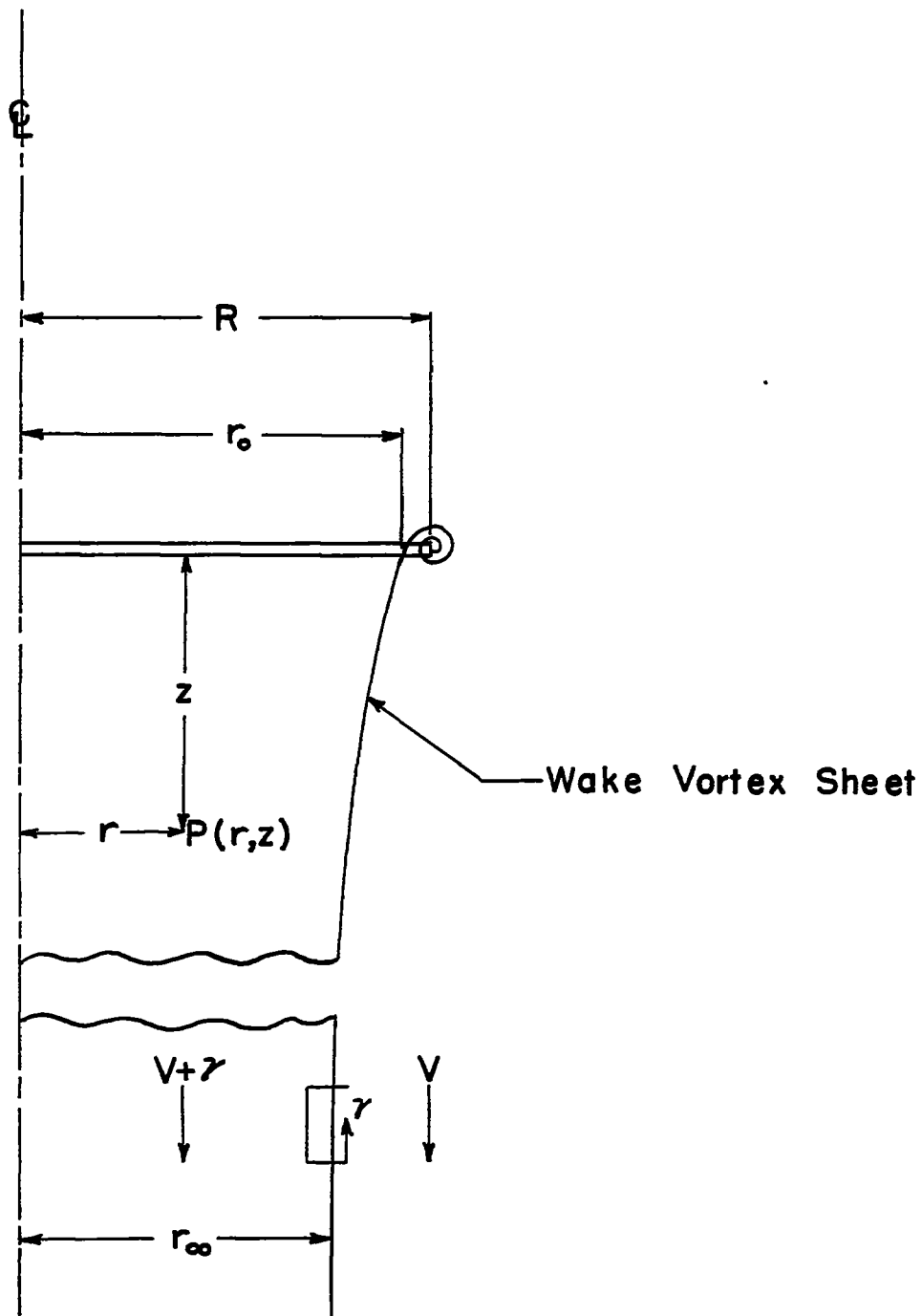


Figure 2.- Schematic section of wake vortex system.

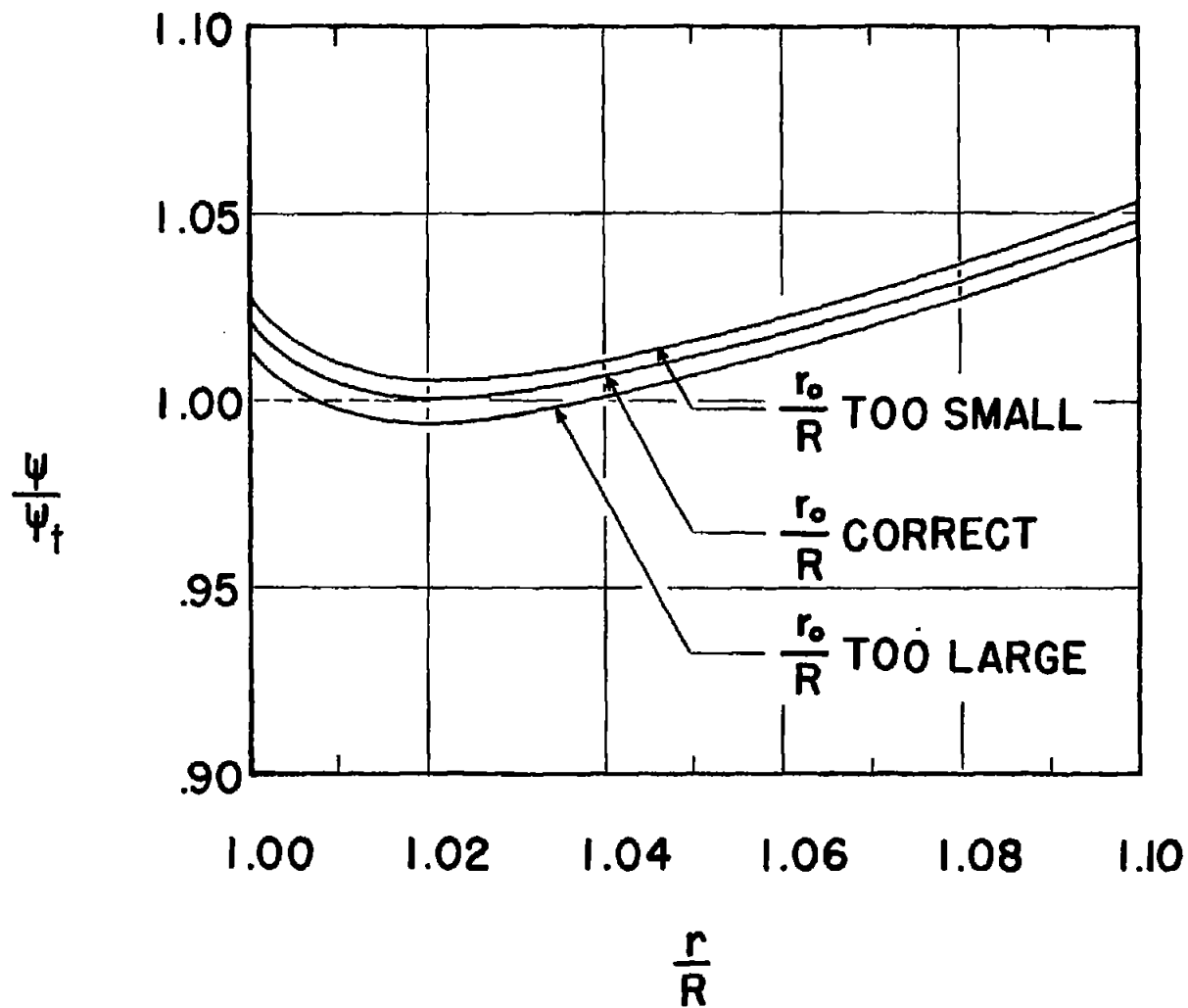


Figure 3.- Illustration of solution for initial wake radius r_0 .

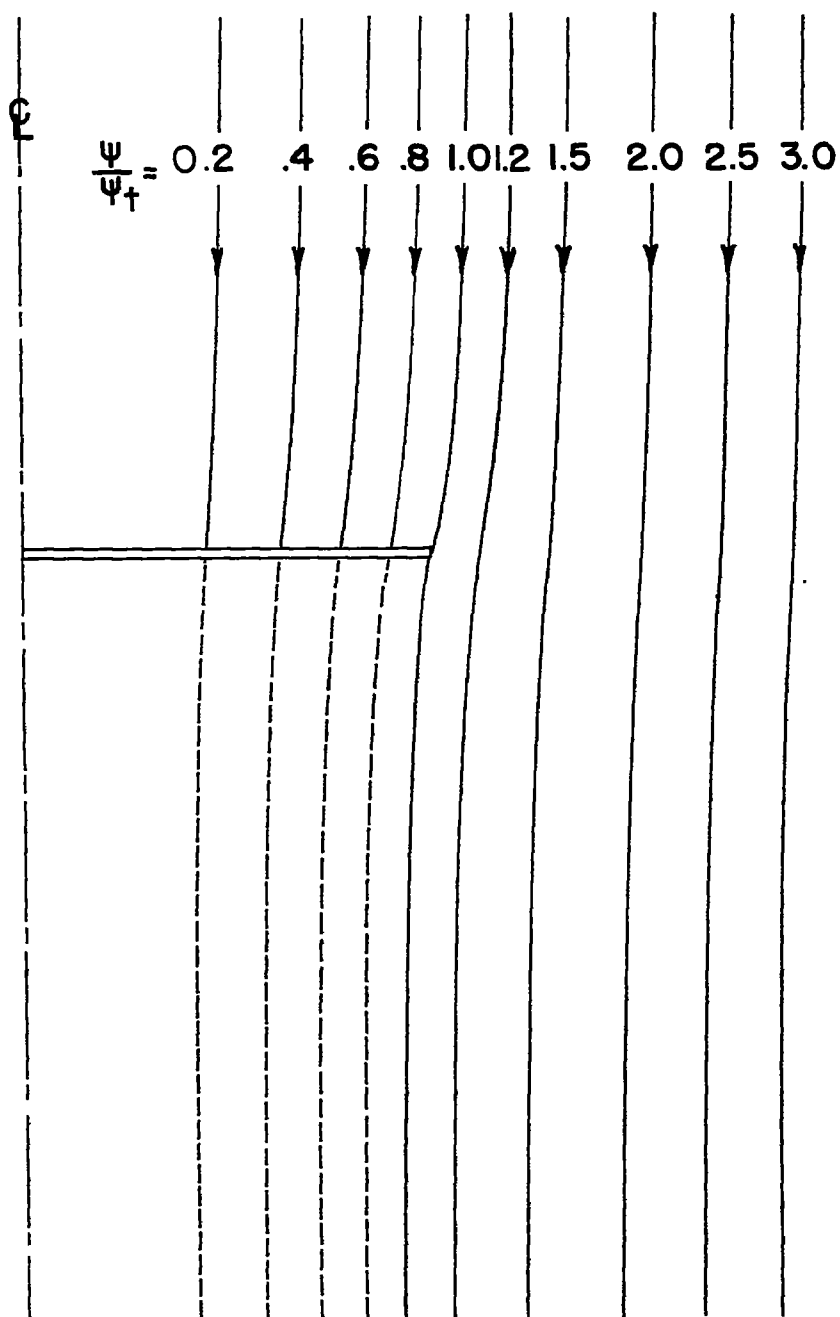
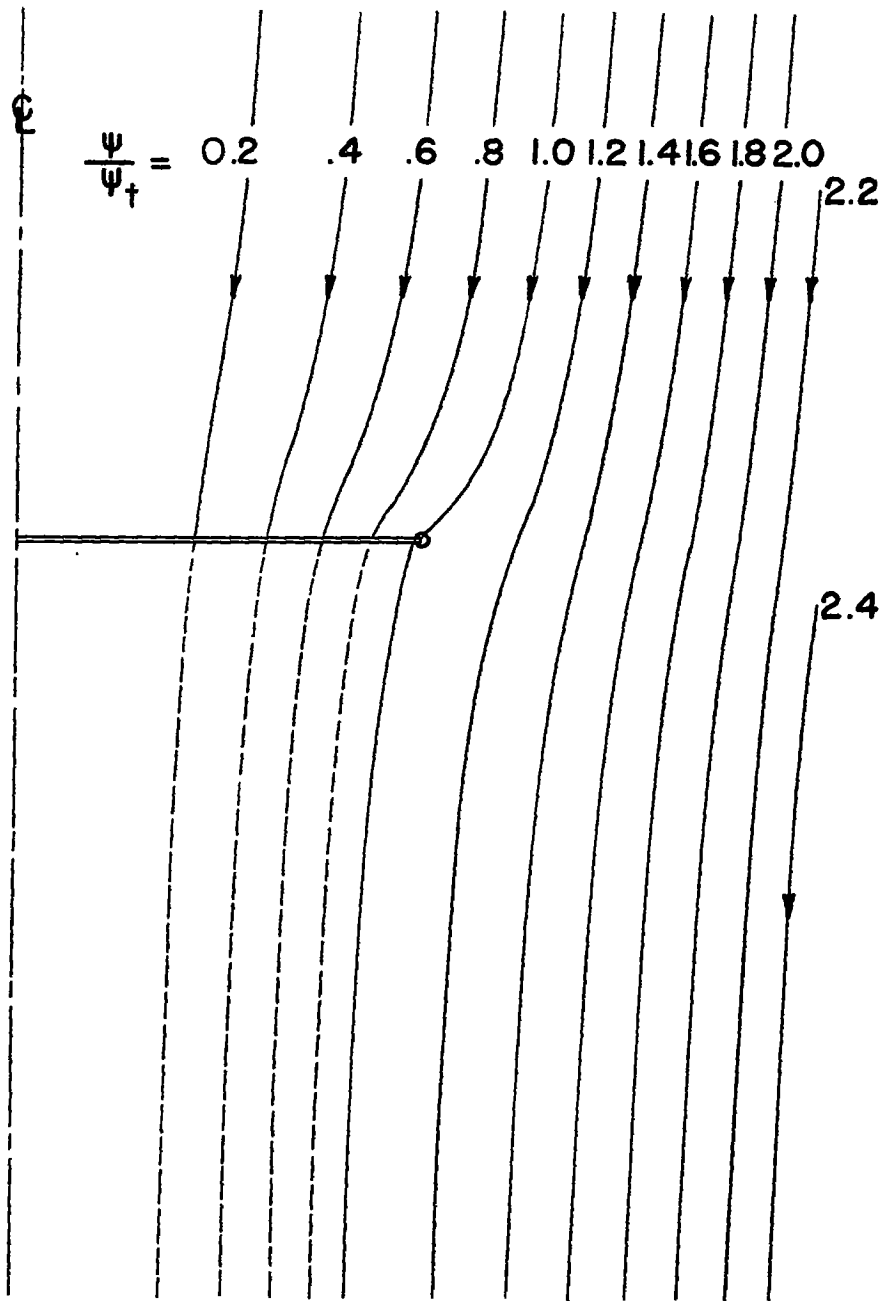
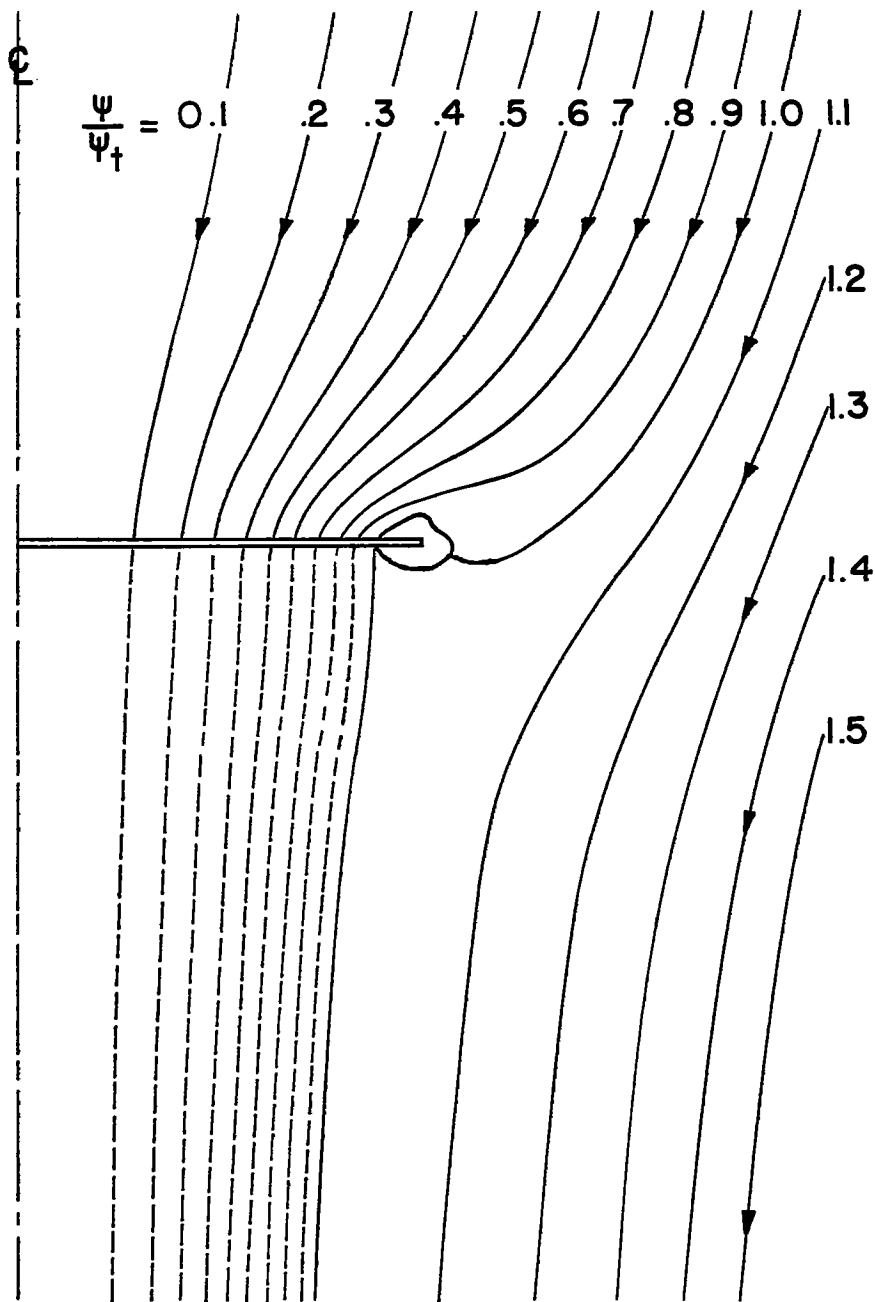
(a) $V = 4v = 2\gamma$.

Figure 4.- Streamlines computed by approximation given in present paper.



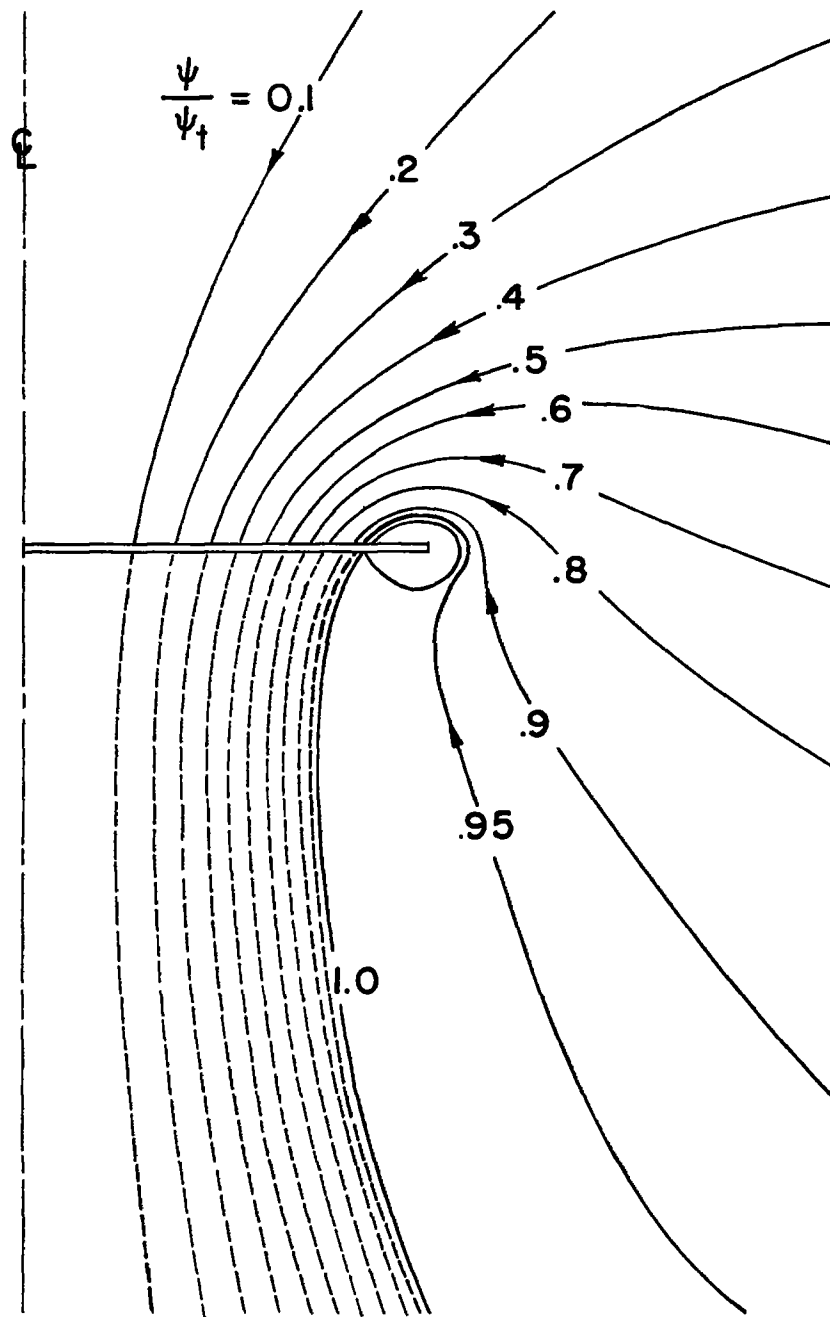
(b) $v = v = \frac{1}{2} \gamma.$

Figure 4.- Continued.



(c) $V = \frac{1}{4} v = \frac{1}{8} \gamma.$

Figure 4.- Continued.



(d) $V = 0$.

Figure 4.- Concluded.

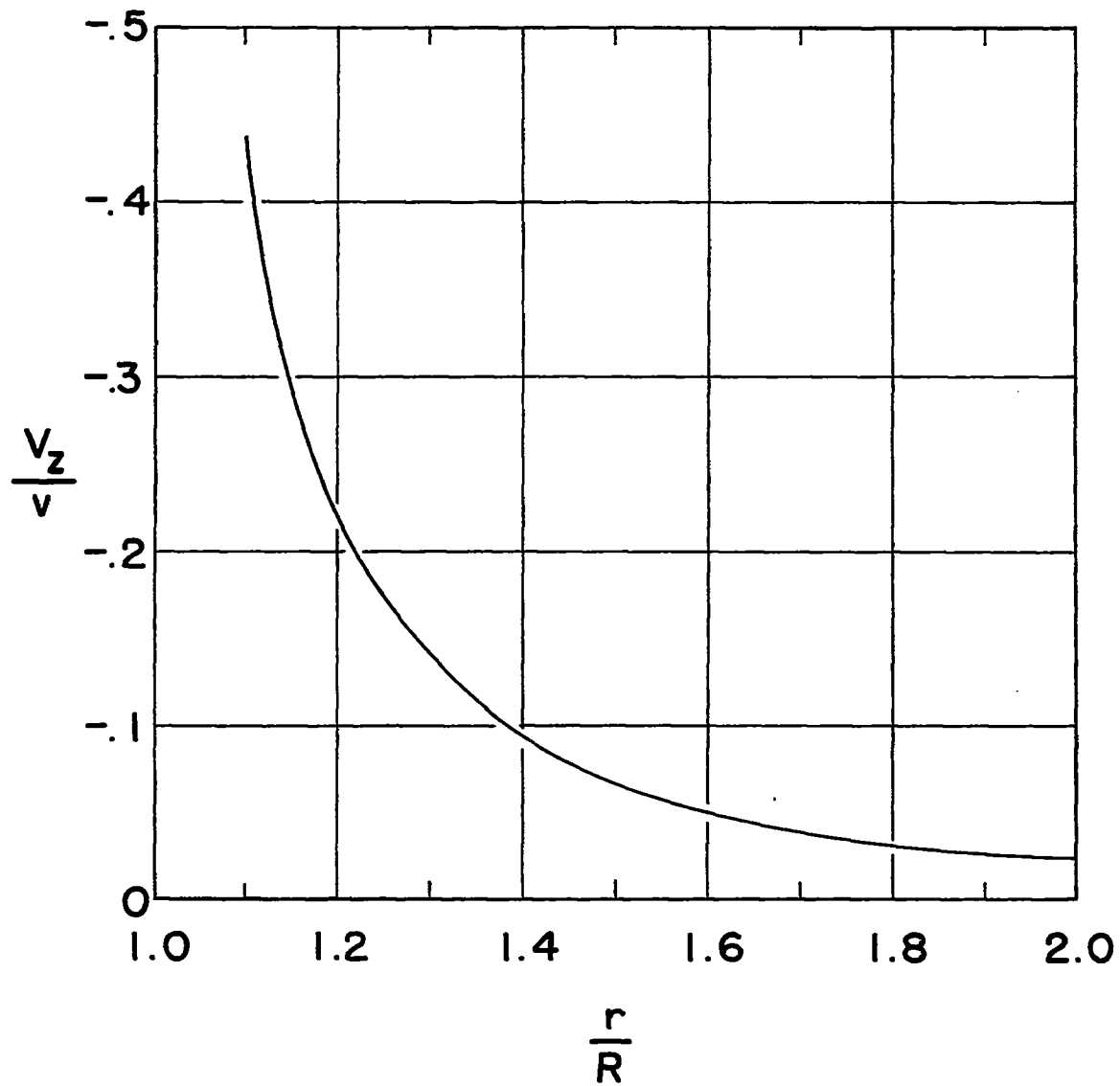


Figure 5.- Normal component of induced velocity in plane of a uniformly loaded, hovering rotor.

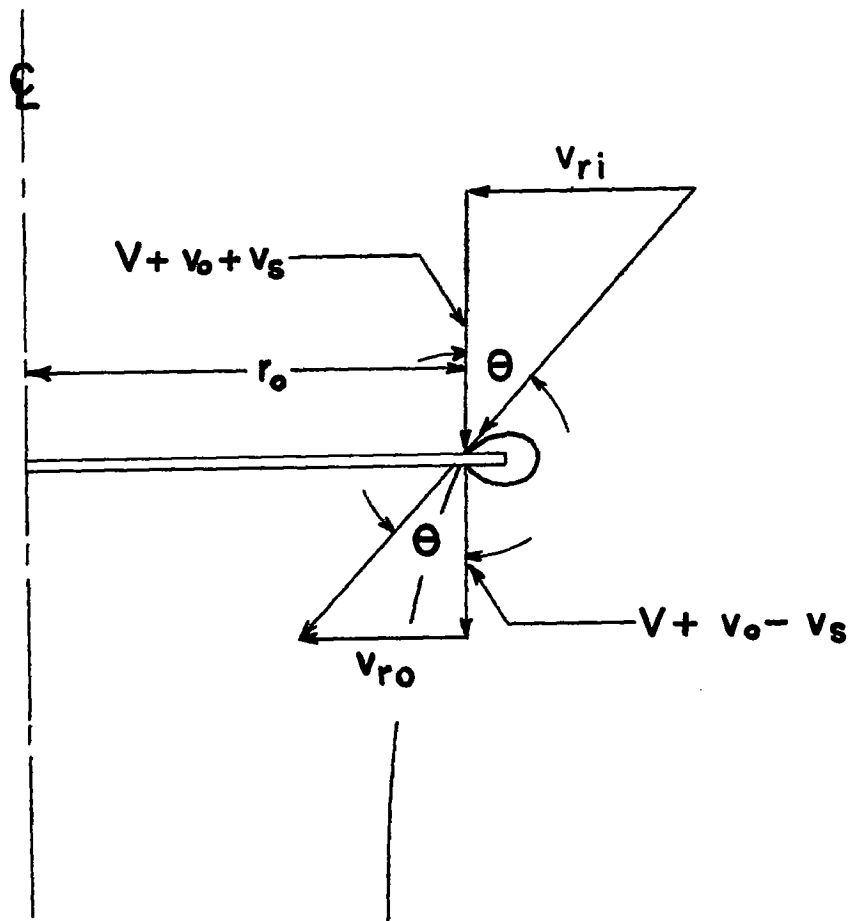


Figure 6.- Velocity diagram at initial wake radius r_0 .

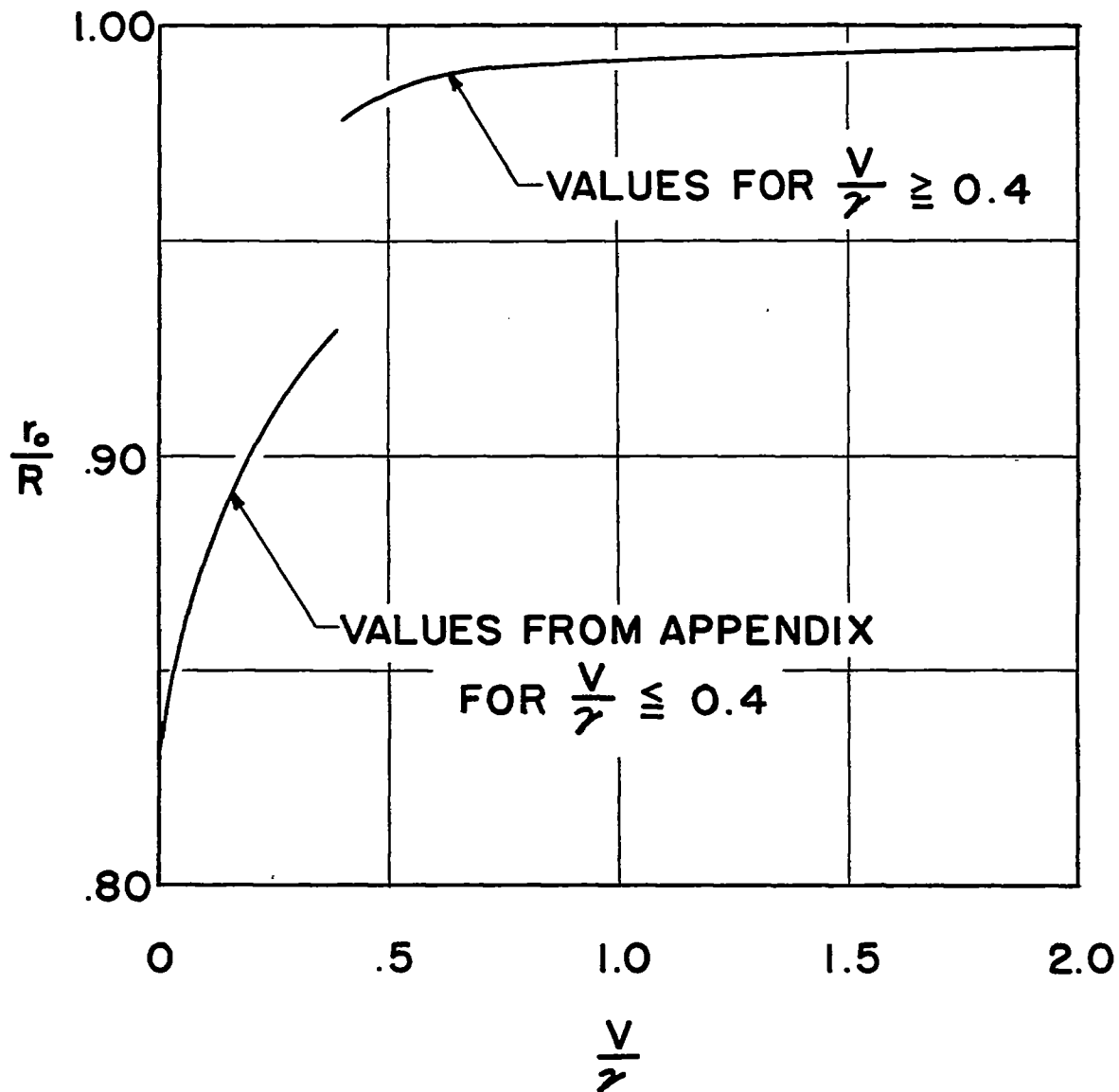


Figure 7.- Values of initial wake radius r_0 .